Proceedings of the 6th International Conference on Recrystallization and Grain Growth (ReX&GG 2016) *Edited by: Elizabeth A. Holm, Susan Farjami, Priyadarshan Manohar, Gregory S. Rohrer, Anthony D. Rollett, David Srolovitz, and Hasso Weiland*
TMS (The Minerals, Metals & Materials Society), 2016

INCONEL 718 MICROSTRUCTURAL EVOLUTION MODELING DURING SEQUENTIAL FORMING STEPS (HOT FORGING FOLLOWED BY RING ROLLING)

O.Beltran[1]

[1]Safran Tech; Rue des Jeunes Bois, Magny-Les-Hameaux, 78772, France

Keywords: Modeling, Inconel 718, Post dynamic recrystallization, ring rolling

Abstract

Inconel 718 industrial hot forging sequences are complex and often composed of several deformation operations at different temperature regimes. The present work focuses on the prediction of the microstructural evolution of Inconel 718 during dynamic (DRX) and post-dynamic recrystallization (PDRX) regimes in the sub-solvus and super-solvus domains. A model coupling the effects of work hardening, recovery, dynamic and post-dynamic recrystallization, and grain growth is presented.

The model has been implemented into a finite element code to calculate the evolution of the microstructure for each integration point of the component mesh file. The predictive capabilities of the model have been compared against a complete industrial forging sequence consisting of hot forging and ring-rolling operations.

Introduction

The tailoring of mechanical properties during hot forming sequences requires an accurate knowledge and control of the microstructural evolution. The modeling of industrial forging sequences of components in Inconel 718 superalloy requires a recrystallization model capable of switching continuously between dynamic (recrystallization during deformation) and post-dynamic mode (recrystallization after deformation) [1-4].

In this paper, a post-dynamic recrystallization model and its coupling to other models describing different metallurgical phenomena is presented. The modeling approach allows the model to handle complex industrial processes such as multi-pass forging and ring rolling. The resulting model was integrated into the finite element software Forge 3D in order to simulate an industrial-type hot forming sequence. The model results were validated at six points of the simulated finite element mesh.

Modeling approach

The proposed microstructural evolution model for Inconel 718 divides forging sequences into three stages: heating, deformation and cooling. At each stage, the microstructural evolution is mostly driven by a specific metallurgical phenomenon.

Grain growth and delta phase evolution model

During the heating stage, the evolution of the microstructure is driven by temperature and the local curvature of the grain boundaries. Normal grain growth is the controlling mechanism. This behavior is described in the model by means of a classical exponential-type law,

$$\frac{d(D^2)}{dt} = \Gamma \eta \exp\left(-\frac{T_0}{T}\right) \tag{1}$$

Where D is the grain size diameter in microns, Γ corresponds to the grain growth kinetics parameter, T_0 grain growth activation temperature and η is an efficiency coefficient dependent on the delta phase concentration. The model used to describe the delta phase evolution kinetics is based on a local equilibrium hypothesis. If the volume fraction is above the equilibrium concentration $X_{\delta eq}$, dissolution takes place at a rate given by,

$$\frac{dX_\delta}{dt} = -K_0 (X_\delta - X_{\delta eq})^2 \exp\left(-\frac{T_\delta}{T}\right) \tag{2}$$

If the volume fraction is below $X_{\delta eq}$, precipitation occurs,

$$dX_\delta = K\sqrt{X_\delta}(X_{\delta eq} - X_\delta)dt \tag{3}$$

Where T_δ is the temperature of maximum precipitation kinetics of the delta phase, K_0 and K are the delta phase dissolution and precipitation kinetics parameters. The influence of the delta phase on the grain growth kinetics has been introduced through the efficiency coefficient η,

$$\eta = 1 - \left(\frac{X_\delta}{X_{\delta 1}^{seuil}}\right)^n \qquad \eta \geq 0 \tag{4}$$

Where $X_{\delta 1}^{seuil}$ is the delta phase fraction threshold and $D_{\delta 1}$ is the delta phase network size.

Work hardening and dynamic recrystallization model

During the deformation stage, the evolution of the microstructure is controlled by work hardening and recovery. Whenever the dislocation density reaches the critical dislocation density of the material, dynamic recrystallization will occur. The model proposed in this work uses the work hardening and dynamic recrystallization models proposed by B. Marty et al. [1]. The evolution of the dislocation density as a function of work hardening and recovery is given by,

$$\dot{\rho} = \rho_0 \cdot B_1 \times \left(\sqrt{\frac{\rho}{\rho_0}}\dot{\varepsilon} - B_2\left(\frac{\rho}{\rho_0} - 1\right)^\beta \times \exp\left(\frac{-T_r}{T}\right)\right) \tag{5}$$

The kinetics of the evolution of the recrystallized fraction during deformation is described through the geometrical interpretation of the necklace-type nucleation hypothesis,

$$\frac{dX}{dt} = A_1 \times \frac{(1-X)^{2/3}}{D_0} \times \exp\left(\frac{-T_x}{T}\right) \times \frac{(\rho - \rho_{cr})}{\rho_0} \quad (6)$$

Where A_1 is the recrystallization kinetics parameter, T_x is the grain boundary mobility activation temperature, ρ is the average dislocation density, ρ_{cr} is the critical dislocation density, and D_0 is the grain size diameter before deformation. As the dynamic recrystallization proceeds, the average non-recrystallized grain size evolves from D_0 to D_{ge} as a function of recrystallized volume fraction,

$$D = D_0(1-X)^{\alpha} + D_{ge}(1-(1-X)^{\alpha}) \quad (7)$$

Where D_{ge} corresponds to the dynamically recrystallized nuclei size and α is a fitting constant.

Post-dynamic recrystallization model

The post-dynamic recrystallization model proposed in this work is based on the following hypotheses:

- After the deformation stage, the microstructure is reclassified in terms of dislocation density.
- At the beginning of post-dynamic recrystallization, the recrystallized volume fraction consists grains with $\rho = \rho_0$. The nuclei driving post-dynamic recrystallization have an initial size defined by the local environment.
- Post-dynamic recrystallization kinetics is based on a volume conservation hypothesis linked to the growth of the reclassified grains. Growth is driven by the temperature and the dislocation density difference between the recrystallized and the deformed grains. As that difference approaches zero, PDRX kinetics tend to normal grain growth kinetics.

If the strain applied during the deformation stage is beyond a critical strain ε_{cr}^{DRX}, the initial microstructure will evolve due to the effect of dynamic recrystallization. As shown in Figure 1a, if the deformation is suddenly stopped, the microstructure in the model is classified into four distinct categories [5]:

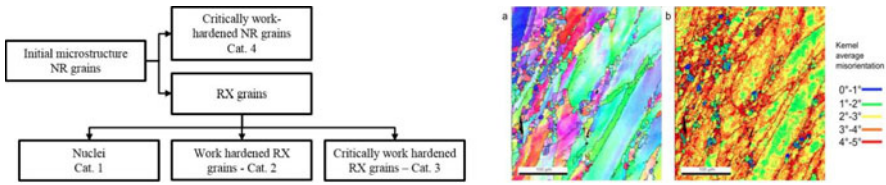

Figure 1. a. Classification categories of grains obtained after deformation. b. Kernel average misorientation map. Quench after deformation at 1000℃ [5].

1. Dynamically recrystallized nuclei with a dislocation density $\rho = \rho_0$
2. Growing dynamically recrystallized grains (RX) with $\rho_0 < \rho < \rho_{cr}$

3. Critically work hardened dynamically recrystallized grains with $\rho > \rho_{cr}$
4. Critically work hardened non-recrystallized grains with $\rho > \rho_{cr}$

At the beginning of post-dynamic recrystallization, the recrystallized fraction consists of grains with a dislocation density $\rho = \rho_0$. The non-recrystallized fraction is a weighted average of the remaining grain categories. This hypothesis is implemented by considering as recrystallized only the nuclei created during the last discrete deformation step $X_{reclass} = \Delta X^{n}_{DRX}$,

$$X^{n}_{DRX} = X^{n-1}_{DRX} + \Delta X^{n}_{DRX} \tag{8}$$

If pinning effects are neglected, the driving force ΔE for grain boundary migration is a function of the stored energy due to the dislocation content and the capillarity term related to the curvature,

$$\Delta E = \tau \Delta \rho + \gamma \Delta \left(\frac{1}{r} \right) \tag{9}$$

where $\tau \approx \mu b^2/2$ is the average energy per unit dislocation length, γ corresponds the energy of the grain boundary per unit area, and r is the grain radius. For the PDRX model it is necessary to determine the size, the number, and the volume fraction of the recrystallized nuclei. The size of the nuclei is calculated through an expression equating the two driving force terms in equation 9. Solving for r and grouping the constant terms in C, the nuclei initial radius is given by,

$$r_{nuclei} = f(\Gamma) \cdot \left(\frac{C}{\rho} \right)^{n} \tag{11}$$

An additional coefficient proportional to the grain growth kinetics parameter $f(\Gamma)$ has been added. The number of initial nuclei is calculated by normalizing $X_{reclass}$ with respect to a unit volume (1 m^3). The number of grains in the unit volume is given by,

$$N_{Grains} = \frac{X_{reclass}}{\left(\frac{4\pi}{3} r^{3}_{nuclei} \right)} \tag{2}$$

The post-dynamic recrystallization kinetics is linked to the growth of nuclei created at the end of the deformation stage and it is given in terms of the volume change of the initial grains with respect to time,

$$\frac{dV}{dt} = A_2 \times (1 - X) \times 4\pi r^2 \exp\left(\frac{-T_x}{T} \right) \times (\rho_{NR} - \rho_0) \cdot \eta \tag{13}$$

where dV is the change in volume, A_2 is the post-dynamic kinetics constant, ρ_{NR} is the average non-recrystallized dislocation density, and η is the efficiency coefficient dependent on the delta

phase volume fraction. After integration, the new volume of each recrystallized grain is the sum of their cumulated volume and the volume change calculated with equation 13,

$$V^* = V + \Delta V \tag{14}$$

Since the initial number of grains N is known, the recrystallized volume fraction is obtained by multiplying the volume of the recrystallized grains by the number of grains,

$$X = NV^* \tag{15}$$

As kinetics is directly related to the volume evolution of recrystallized grains, the post-dynamically recrystallized grain size diameter is given by,

$$D = 2 \times \sqrt[3]{\frac{3V^*}{4\pi}} \tag{16}$$

Once a recrystallized fraction of 90% is reached, it is assumed that the behavior is closer to that of normal grain growth. At this time, the model switches to the normal grain growth model expression with the same parameters and equations used during the heating stage.

Results and discussion

The model was implemented into the finite element software Forge® via post-processing user subroutines. To simulate ring rolling operations, Forge® 3D makes use of a fixed structured mesh [6]. A detailed analysis showed several abnormalities in the temperature, strain and strain rate variables transfer from the software to the user routines during ring rolling simulations.

In order to solve the variable transfer issue and validate the model, the real thermomechanical history calculated by Forge® was extracted through six lagrangian sensors and used as input on a stand-alone version of the model. All the state variables calculated are continuous throughout the whole sequence.

The grain size results predicted by the model were compared against an industrial test case composed of a forging operation consisting of three forging strokes in the sub-solvus regime followed by a ring rolling operation in the super-solvus regime. The component was cooled to room temperature between the forging and ring rolling operations.

The predicted grain size at each sensor position was compared to that observed in the component cut-up at the end of the ring rolling operation. Measured grain sizes were determined through optical microscopy using ASTM Standard E112. The results are presented in Table I. The results predicted by the model present a relatively good agreement with the measured grain sizes. For most of the points measured, the model slightly underestimates the grain size. A parametric analysis showed that this is due to the influence of the delta phase on grain growth.

Table I. Predicted and measured average grain size in ASTM Standard E112 [7] at the end of the ring rolling operation (20°C).

		Ring Rolling Operation	
	Position	Predicted [ASTM]	Measured [ASTM]
Sensor 1	Outer surface	11.26	11.50
Sensor 2	Outer surface	12.12	11.50
Sensor 3	Center	10.99	10.50
Sensor 4	Center	9.76	8.50
Sensor 5	Inner surface	11.95	12.00
Sensor 6	Inner surface	12.54	12.00

Conclusions

A microstructural evolution model for Inconel 718 during industrial sequences based on the coupling of grain growth, dynamic recrystallization and a new post-dynamic recrystallization model is presented. Comparison with grain size measurements show that the proposed model is capable of predicting the microstructural evolution trends during complex forming sequences, including ring rolling. In order to improve the results, a first analysis suggests that the delta phase precipitation model needs to be revised and improved.

References

[1] B. Marty et al., "Recrystallization and work-hardening prediction during forging process of Inconel 718", Superalloys 718, 625, 706 and various derivatives, Edited by E.A. Loria, The Minerals, Metals & Materials Society, 1997.

[2] J.P. Thomas et al, "EBSD Investigation and modeling of the microstructural evolutions of superalloy 718 during hot deformation", Superalloys 2004, Edited by K.A. Green, T.M. Pollock, H. Harada, The Minerals, Metals & Materials Society, 2004.

[3] M. Zouari et al., "Multi-pass forging of Inconel 718 in the delta supersolvus domain: assessing and modeling microstructure evolution", MATEC Web of conferences 14, 12001, 2014

[4] K. Subrammanian, H.P. Cherukuri, "Prediction of microstructure evolution during multi-stand shape rolling of nickel-base superalloys", *Integration Materials and Manufacturing Innovation*, 2014, 3:27

[5] O. Beltran, K. Huang, R.E. Logé, "A mean field model of dynamic and post-dynamic recrystallization predicting kinetics, grain size and flow stress," *Computational Materials Science*, 102 (2015), 293-303.

[6] Transvalor SA, Forge 2011: Forging Simulation Software Reference documentation Part 3: Meshing, 36-37.

[7] ASTM E112-13, Standard Test Methods for Determining Average Grain Size, ASTM International, West Conshohocken, PA, 2013, www.astm.org